JOURNAL OF OPTIMIZATION THEORY AND APPLICATIONS: Vol. 110, No. 3, pp. 557–583, September 2001 (© 2001)

Generalized Homotopy Approach to Multiobjective Optimization[1]

C. HILLERMEIER[2,3]

Communicated by W. Stadler

Abstract. This paper proposes a new generalized homotopy algorithm for the solution of multiobjective optimization problems with equality constraints. We consider the set of Pareto candidates as a differentiable manifold and construct a local chart which is fitted to the local geometry of this Pareto manifold. New Pareto candidates are generated by evaluating the local chart numerically. The method is capable of solving multiobjective optimization problems with an arbitrary number k of objectives, makes it possible to generate all types of Pareto optimal solutions, and is able to produce a homogeneous discretization of the Pareto set. The paper gives a necessary and sufficient condition for the set of Pareto candidates to form a $(k-1)$-dimensional differentiable manifold, provides the numerical details of the proposed algorithm, and applies the method to two multiobjective sample problems.

The reason why the Pareto candidate forms a k-1 dimensional differentiable manifold is that one of the k objectives is being inspected as a dependent variable and the other k-1 objectives are being considered as the independent variables so that they forms a k-1 objectives which leads the inspected objectives to move

Key Words. Vector optimization problems, Pareto-optimal solutions, differentiable manifolds, homotopy methods.

1. Introduction

The task of optimizing the design or status of some real-world system often requires assessing the system performance according to multiple criteria, which typically compete with each other; see e.g. Ref. 1. Combining

[1]The author expresses his gratitude to Prof. Dr. Dr.h.c. Karl-Heinz Hoffmann for helpful discussions and valuable support. A fruitful hint of Prof. Dr. Klaus Ritter concerning Theorem 2.3 is gratefully acknowledged. Dr. Reinhart Schultz has provided the first (academic) multiobjective sample problem. The work has been supported by the German "Bundesministerium für Bildung und Forschung" in the framework of Project LEONET.

[2]Associate Professor, Institute of Applied Mathematics, Friedrich Alexander University of Erlangen-Nuremberg, Erlangen, Germany.

[3]Principal Research Scientist, Corporate Technology, Siemens AG, Munich, Germany.

0022-3239/01/0900-0557$19.50/0 © 2001 Plenum Publishing Corporation

the k individual real-valued objectives in one vector-valued objective function $f: \mathbb{R}^n \to \mathbb{R}^k$, $x \mapsto f(x)$, the arising multicriteria or multiobjective optimization problem can be posed as follows:

$$\text{(MOP)} \quad \min_{x \in R} \{ f(x) \}, \qquad R := \{ x \in \mathbb{R}^n \mid h(x) = 0, g(x) \leq 0 \}, \tag{1}$$

where $h: \mathbb{R}^m \to \mathbb{R}^m$, $m \leq n$, and $g: \mathbb{R}^n \to \mathbb{R}^q$. In this paper, we investigate multiobjective optimization problems where only equality constraints are present and where f and h are twice continuously differentiable mappings. Since minimization requires some comparison concept, we define the following order in $\mathbb{R}^k$.

Definition 1.1. Consider two vectors, v, $w \in \mathbb{R}^k$. The vector v is called less than or equal to w, $v \leq_p w$, if $v_i \leq w_i$ for all $i \in \{1, \ldots, k\}$.

As two arbitrary vectors v, $w \in \mathbb{R}^k$ are not necessarily comparable to each other with respect to $\leq_p$, the relation $\leq_p$ establishes only a partial order in $\mathbb{R}^k$. This partial order makes it possible to define the concept of Pareto optimality, which states more precisely what is meant by a solution to the multicriteria optimization problem (MOP).

Definition 1.2. Consider the multiobjective optimization problem (MOP). A point $x^* \in R \subseteq \mathbb{R}^n$ is called an efficient point or a Pareto optimal solution if there does not exist any $u \in R$ with $f(u) \neq f(x^*)$ and $f(u) \leq_p f(x^*)$.

If the above condition is checked only for feasible points within some open neighborhood $U(x^*) \in \mathbb{R}^n$ of x^*, then x^* is called locally efficient or a local Pareto-optimal solution. All deterministic computational methods for general nonlinear multiobjective optimization, including the one presented in this paper, can at best guarantee the local Pareto optimality of the obtained solution(s). Thus, the term ''Pareto optimality'' will henceforth mean ''local Pareto optimality''. Since the Pareto optimal solutions of (MOP) are not unique in general, the desired solution of (MOP) is the entire Pareto optimal set or at least a whole collection of Pareto optimal points which is representative of the entire spectrum of efficient solutions.

Virtually all deterministic approaches for the numerical solution of (MOP) are based on the idea of transforming the original multiobjective optimization problem into some problem of scalar-valued optimization. In general, as the solution of each scalar-valued substitute problem yields only a single efficient point, a whole parametrized family of transformations is constructed. Then, the change of the transformation parameter makes it

possible to generate different scalar-valued substitute problems, giving the chance to generate different efficient solutions.

Classical approaches employing this principle are the weighting method (see Ref. 2), which forms a weighted sum of the individual objectives (the vector of weights serving as a transformation parameter) and the ϵ-constraint method (see Ref. 3), which selects one of the individual objectives for scalar minimization, determining the maximum values for the remaining objectives. A recent technique called normal-boundary intersection bases a scalarization of (MOP) on the following geometrical observation (see Refs. 4–5): The image $f(x^*)$ of an efficient point x^* is the intersection of the normal emanating from any point of a certain simplex in $\mathbb{R}^k$ and the boundary of the image $f(R)$ of the feasible set. The problem of calculating this intersection point can be formulated as a scalar-valued optimization problem.

The close relation between (MOP) and parametrized optimization problems leads naturally to the idea of employing continuation-type techniques for the solution of (MOP). Indeed, Rakowska et al. (Ref. 6) have suggested such an approach; however, their suggestion suffers from two severe drawbacks. By construction, their approach can be applied only to bicritical problems; also their method determines only a certain type of Pareto optimal solutions, namely those points which minimize some weighted sum of the objectives.

In this paper, we present a generalized homotopy method avoiding these disadvantages. The principal idea is to consider the set of Pareto candidates as a differentiable manifold and to construct a local chart which is fitted to the local geometry of that Pareto manifold (see Ref. 7). The proposed homotopy approach generates new Pareto candidates by evaluating the local chart numerically. The method is capable of solving (MOP) with an arbitrary number k of objectives, makes it possible to generate all types of Pareto optimal solutions, and is able to produce a homogeneous discretization of the Pareto set.

The paper is organized as follows. Section 2 analyzes the manifold of Pareto candidates from the viewpoint of differential geometry. First, a necessary and sufficient condition for the set of Pareto candidates to form a $(k-1)$-dimensional differentiable manifold is given. A corollary interprets this condition with respect to scalar optimization theory. The local chart which forms the basis of our homotopy approach is constructed in Section 2.3. Section 3 provides the numerical details of the proposed method, including a proof of the homogeneous discretization property. Finally, Section 4 demonstrates the way in which the method works by solving numerically two multiobjective sample problems.

2. Manifold of Pareto Candidates

2.1. Connection to Scalar Optimization. The following important theorem of Kuhn and Tucker gives a necessary condition or Pareto optimality, thereby forging a link between vector optimization and scalar optimization; for proof, see Ref. 8.

Theorem 2.1. Let x^* be Pareto optimal with respect to (MOP). Let $h(x)$ comply with the following constraint qualification:

(CQ) the set of vectors $\{\nabla h_i(x^*) \mid i = 1, \ldots, m\}$ are linearly independent.

Then, there exist vectors $\lambda \in \mathbb{R}^m$ and $\alpha \in \mathbb{R}^k$, with $\alpha_i \geq 0$, $i = 1, \ldots, k$, and $\sum_{i=1}^{k} \alpha_i = 1$, such that

$$\sum_{i=1}^{k} \alpha_i \nabla f_i(x^*) + \sum_{j=1}^{m} \lambda_j \nabla h_j(x^*) = 0, \tag{2}$$

$$h_i(x^*) = 0, \qquad i = 1, \ldots, m. \tag{3}$$

We define the scalar-valued function

$$g_\alpha : \mathbb{R}^n \to \mathbb{R}, \qquad x \mapsto g_\alpha(x) := \sum_{i=1}^{k} \alpha_i f_i(x),$$

and note that, due to

$$\sum_{i=1}^{k} \alpha_i \nabla f_i(x) = \nabla g_\alpha(x),$$

Eqs. (2) and (3) are equivalent to the proposition that the efficient point x^* meets the first-order necessary condition for a local extremum of g_α subject to $h(x) = 0$. The mapping g_α is a convex combination of the individual objectives f_i, and each coefficient α_i represents the relative weight of f_i within g_α. Since the weighting method calculates the minima of convex combinations g_α, it is based on the above result of Kuhn and Tucker. In general, this approach does not yield the complete Pareto set, because the second-order necessary condition for a point x^* to be a local minimizer of g_α is not necessary for x^* to be a Pareto optimal solution of the corresponding (MOP). The missing second-order necessary condition distinguishes multiobjective optimization from scalar-valued optimization and may be considered to be the price which has to be paid for the weak order concept in $\mathbb{R}^k$ (partial order as opposed to the total order of $\mathbb{R}$). In multiobjective optimization problems where the image $f(R)$ of the feasible set is not convex,

saddle points of convex combinations g_α may form an essential part of the set of Pareto optimal solutions; for a detailed discussion, see Ref. 7.

2.2. Criteria for the Rank Condition. Due to the Kuhn–Tucker theorem, for each Pareto optimum x^* meeting the constraint qualification (CQ), there exists a vector $(x^*, \lambda^*, \alpha^*) \in \mathbb{R}^n \times \mathbb{R}^m \times \mathbb{R}^k_+$ which solves the following nonlinear system of equations:

$$F(x, \lambda, \alpha) = 0, \tag{4}$$

where the function F: $\mathbb{R}^{n+m+k} \to \mathbb{R}^{n+m+1}$ is defined by

$$F(x, \lambda, \alpha) := \begin{bmatrix} \sum_{i=1}^{k} \alpha_i \nabla f_i(x) + \sum_{j=1}^{m} \lambda_j \nabla h_j(x) \\ h(x) \\ \sum_{i=1}^{k} \alpha_l - 1 \end{bmatrix}. \tag{5}$$

In the sequel, we will consider an important subset of these solutions, namely, the set of candidates for Pareto optimality,

$$M := \{(x^*, \lambda^*, \alpha^*) \in \mathbb{R}^{n+m+k} \,|\, F(x^*, \lambda^*, \alpha^*) = 0 \text{ and } \alpha_i^* > 0, i = 1, \ldots, k\}.$$

Our approach is based on the idea to characterize the points of M by suitable local charts; see Section 2.3 below. The existence of local charts with the same dimension at any point of M is guaranteed if M is a $(k-1)$-dimensional C^1-manifold. The following theorem clarifies under which conditions this is the case.

Theorem 2.2. Consider the set

$$M := \{(x^*, \lambda^*, \alpha^*) \in \mathbb{R}^{n+m+k} \,|\, F(x^*, \lambda^*, \alpha^*) = 0 \text{ and } \alpha_i^* > 0, i = 1, \ldots, k\},$$

where $F \in C^1(\mathbb{R}^{n+m+k}, \mathbb{R}^{n+m+1})$ is defined according to (5). Now let $(x^*, \lambda^*, \alpha^*) \in M$ be a point complying with the following rank condition:

$$\text{rank } F'(x^*, \lambda^*, \alpha^*) = n + m + 1, \tag{6}$$

where $F'(x^*, \lambda^*, \alpha^*)$ denotes the Jacobian matrix of F. Then, there exists an open neighborhood $U \subset \mathbb{R}^{n+m+k}$ of $(x^*, \lambda^*, \alpha^*)$ such that $M \cap U$ is a $(k-1)$-dimensional C^1-submanifold of $\mathbb{R}^{n+m+k}$, and therefore a $(k-1)$-dimensional C^1-manifold.

Proof. The full rank of the matrix $F'(x^*, \lambda^*, \alpha^*)$ implies that there exists a $(n+m+1) \times (n+m+1)$ submatrix A of $F'(x^*, \lambda^*, \alpha^*)$ with $\det A \neq 0$.

Due to the continuity of the mapping $F': \mathbb{R}^{n+m+k} \to \mathbb{R}^{n+m+1} \times \mathbb{R}^{n+m+k}$, $(x, \lambda, \alpha) \mapsto F'(x, \lambda, \alpha), \det A$ considered as a real-valued function of (x, λ, α) is continuous as well, and there exists an open neighborhood U of $(x^*, \lambda^*, \alpha^*)$ where $\det A \neq 0$ holds. As a consequence, the rank condition (6) is fulfilled by all points in U. Now, the proposition follows immediately from the definition of a $(k-1)$-dimensional C^1-submanifold of $\mathbb{R}^{n+m+k}$. □

In order to work out a necessary and sufficient condition for the fulfillment of the crucial rank condition (6), some preparatory remarks are appropriate.

We assume that, at the point x^*, the equality constraints $h(x) = 0$ comply with the constraint qualification (CQ). then, the equality constraints define, within an open neighborhood $V \subset \mathbb{R}^n$ of x^*, an $(n-m)$-dimensional submanifold of $\mathbb{R}^n$, the constraint surface. Its tangent space is an $(n-m)$-dimensional linear subspace of $\mathbb{R}^n$, which can be written as the orthogonal complement $S^\perp$ of the subspace $S \subset \mathbb{R}^n$ defined by

$$\text{span}\,\{\nabla h_1(x^*), \ldots, \nabla h_m(x^*)\}.$$

The Jacobian matrix $F'(x^*, \lambda^*, \alpha^*)$, whose rank is under investigation, has an important $n \times n$ submatrix

$$\nabla^2 L_{\alpha^*}(x^*) := \nabla_x^2 (\alpha^{*T} f(x) + \lambda^{*T} h(x))\big|_{x = x^*},$$

that is the Hessian with respect to x of the Lagrangian $L_{\alpha^*}(x, \lambda)|_{\lambda = \lambda^*}$ of the scalar-valued objective function g_{α^*}. Restricting this linear mapping to the subspace $S^\perp$ gives a linear mapping $\nabla^2 L_{\alpha^*}(x^*)|_{S^\perp}$ defined by

$$\nabla^2 L_{\alpha^*}(x^*)\big|^{S^\perp}: \begin{cases} S^\perp \to S^\perp, \\ t \mapsto P_{S^\perp} \nabla^2 L_{\alpha^*}(x^*) t, \end{cases} \tag{7}$$

where $P_{S^\perp}$ stands for the projector onto $S^\perp$. The matrix representation of $\nabla^2 L_{\alpha^*}(x^*)|_{S^\perp}$ with respect to an arbitrary orthogonal basis of $S^\perp$ is symmetric. Hence, $S^\perp$ can be spanned by an orthonormal basis consisting of eigenvectors of $\nabla^2 L_{\alpha^*}(x^*)|_{S^\perp}$, and all the eigenvalues $\nu_1, \ldots, \nu_{n-m}$ are real numbers.

Now, we are able to put the rank condition (6) in the following way.

Theorem 2.3. Consider a point $(x^*, \lambda^*, \alpha^*) \in M$, and assume that, at the point $x^* \in \mathbb{R}^n$, the constraint qualification (CQ) is fulfilled. Then, the

following equivalence holds:

$$\begin{aligned}&\operatorname{rank} F'(x^*, \lambda^*, \alpha^*) = n + m + 1\\ &\Leftrightarrow E := \{u \in S^{\perp} \mid u \in \operatorname{kernel} f'(x^*) \text{ and}\\ &\qquad u \in \{\text{eigenspace corresponding to the eigenvalue 0 of}\\ &\qquad\quad \nabla^2 L_{\alpha^*}(x^*)|_{S^{\perp}}\}\} = \varnothing.\end{aligned}$$

Proof. First, we note that $\operatorname{rank} F'(x^*, \lambda^*, \alpha^*) = n + m + 1$ is equivalent to saying that the linear equation

$$F'(x^*, \lambda^*, \alpha^*)^T z = 0 \tag{8}$$

has only the trivial solution $z_0 = 0 \in \mathbb{R}^{n+m+1}$.

($\Leftarrow$) We start by a closer look at (8). Differentiating the function F results in

$$F'(x^*, \lambda^*, \alpha^*)^T = \left[\begin{array}{c|c|c} \nabla^2 L_{\alpha^*}(x^*) & \nabla h_1(x^*) \ldots \nabla h_m(x^*) & 0 \\ \hline \nabla h_1(x^*)^T & & \\ \vdots & 0 & 0 \\ \nabla h_m(x^*)^T & & \\ \hline \nabla f_1(x^*)^T & & 1 \\ \vdots & 0 & \vdots \\ \nabla f_k(x^*)^T & & 1 \end{array}\right]. \tag{9}$$

Writing a solution vector $z \in \mathbb{R}^{n+m+1}$ as

$$z = \begin{bmatrix} a \\ b \\ c \end{bmatrix},$$

with $a \in \mathbb{R}^n$, $b \in \mathbb{R}^m$, $c \in \mathbb{R}$, we get a linear system of equations which is equivalent to (8):

$$\nabla^2 L_{\alpha^*}(x^*)a = -Hb, \text{ where } H := (\nabla h_1(x^*) \ldots \nabla h_m(x^*)) \in \mathbb{R}^{n \times m}, \quad (10)$$

$$\nabla h_1(x^*)^T a = 0, \quad (11a)$$

$$\vdots$$

$$\nabla h_m(x^*)^T a = 0, \quad (11b)$$

$$\nabla f_1(x^*)^T a = -c, \quad (12a)$$

$$\vdots$$

$$\nabla f_k(x^*)^T a = -c. \quad (12b)$$

Equations (11) are equivalent to $a \in S^\perp$, and Eqs. (12) lead to the conclusion that

$$\nabla g_{\alpha^*}(x^*)^T a \equiv \sum_{i=1}^{k} \alpha_i^* \nabla f_i(x^*)^T a = -c \sum_{i=1}^{k} \alpha_i^* = -c. \quad (13)$$

Since $F(x^*, \lambda^*, \alpha^*) = 0$, we have $\nabla g_{\alpha^*}(x^*) \in S$. On the other hand, $a \in S^\perp$, so we conclude that $c = 0$. Thus, Eqs. (12) imply that $f'(x^*)a = 0$, or equivalently, $a \in \text{kernel } f'(x^*)$.

The columns of H span the subspace image $H \subset \mathbb{R}^n$. On the other hand, they form a basis of S thanks to the constraint qualification (CQ). Thus, we conclude that image $H = S$. Therefore, applying the projector $P_{S^\perp}$ to Eq. (10) results in

$$P_{S^\perp} \nabla^2 L_{\alpha^*}(x^*)a = -P_{S^\perp} Hb = 0.$$

Since a is a vector of $S^\perp$, this is equivalent to

$$\nabla^2 L_{\alpha^*}(x^*)|_{S^\perp} a = 0;$$

i.e., a is an eigenvector belonging to the eigenvalue 0 of $\nabla^2 L_{\alpha^*}(x^*)|_{S^\perp}$.

Having provided the material needed, we now assume that the set E as defined in the proposition is empty and that Eq. (8) has a nontrivial solution $z \neq 0$. The latter assumption implies $a \neq 0$, since $a = 0$ would lead to $b = 0$ [according to (10), the vector $-b$ can be considered as the vector of coefficients of $\nabla^2 L_{\alpha^*}(x^*)a \in S$ with respect to the basis $\{\nabla h_1(x^*), \ldots, \nabla h_m(x^*)\}$ of S], and since $c = 0$ holds anyway. Thus, $a \in S^\perp$ is an element of E conflicting with the assumption that E is empty. Hence, the direction ($\Leftarrow$) is proven.

($\Rightarrow$) We suppose that (8) has only the trivial solution $z_0 = 0$ and that there is a vector $u \in E$, $u \neq 0$. Consider the vector

$$z = \begin{bmatrix} u \\ v \\ 0 \end{bmatrix} \in \mathbb{R}^{n+m+1},$$

where $-v$ is the (uniquely determined) vector of coefficients of $\nabla^2 L_{\alpha^*}(x^*)u \in S$ with respect to the basis $\{\nabla h_1(x^*), \ldots, \nabla h_m(x^*)\}$ of S. By construction, the triple

$$\begin{bmatrix} u \\ v \\ 0 \end{bmatrix}$$

solves the system of Eqs. (10)–(12). Therefore, z is a nontrivial solution of (8). Due to this contradiction, the assumption that there is a nontrivial vector $u \in E$ cannot be true. □

In order to clarify the meaning of the given criterion for the fulfillment of the rank condition (6), we now interpret it from the viewpoint of scalar optimization. First, recall that $(x^*, \lambda^*, \alpha^*) \in M$ means that x^* meets the first-order necessary condition for a local extremum of the objective function g_{α^*} subject to $h(x) = 0$. For a classification of the stationary points x^* of g_{α^*} by means of second-order conditions, the linear mapping $\nabla^2 L_{\alpha^*}(x^*)|_{S^\perp}$ plays a role which is entirely analogous to that of the Hessian of the objective function in the unconstrained case; see e.g. Ref. 9. $\nabla^2 L_{\alpha^*}(x^*)|_{S^\perp}$ is regular if and only if all eigenvalues $\nu_1, \ldots, \nu_{n-m}$ are nonzero. Thus, we can state as a corollary of Theorem 2.3 that the regularity of $\nabla^2 L_{\alpha^*}(x^*)|_{S^\perp}$ is a sufficient criterion for the rank condition (6). In the context of scalar optimization, the regularity of $\nabla^2 L_{\alpha^*}(x^*)|_{S^\perp}$ means that an analysis of its eigenvalues makes it possible to decide whether a stationary point x^* is a local minimum, a saddle point, or a local maximum of the objective function g_{α^*} subject to $h(x) = 0$:

(a) $\nu_i > 0, \forall i = 1, \ldots, n-m \Leftrightarrow \nabla^2 L_{\alpha^*}(x^*)|_{S^\perp}$ is positive definite, and x^* is an isolated minimum point of g_{α^*} subject to $h(x) = 0$.

(b) $\exists (i, j) \in \{1, \ldots, n-m\} \times \{1, \ldots, n-m\}$ such that $\nu_i > 0$ and $\nu_j < 0$. In that case, $\nabla^2 L_{\alpha^*}(x^*)|_{S^\perp}$ is regular and indefinite, and x^* is a saddle point of g_{α^*} subject to $h(x) = 0$.

(c) $\nu_i < 0, \forall i = 1, \ldots, n-m \Leftrightarrow \nabla^2 L_{\alpha^*}(x^*)|_{S^\perp}$ is negative definite, and x^* is an isolated maximum point g_{α^*} subject to $h(x) = 0$.

While case (c) does not lead to Pareto optimal points, cases (a) and (b) result in the following corollary of Theorem 2.3.

Corollary 2.1. Consider a point $(x^*, \lambda^*, \alpha^*) \in M$ and assume that, at the point $x^* \in \mathbb{R}^n$, the constraint qualification (CQ) is fulfilled. Let $x^* \in \mathbb{R}^n$ be either a local minimum point of g_{α^*}, subject to $h(x) = 0$, meeting the second-order sufficient condition for optimality, or a saddle point of g_{α^*},

subject to $h(x) = 0$, such that $\nabla^2 L_{\alpha^*}(x^*)|_{S^\perp}$ is regular and indefinite. Then, rank $F'(x^*, \lambda^*, \alpha^*) = n + m + 1$.

Now, one may ask what happens at the borderline between minimum point and saddle point. To be more precise, let us consider two points, $(x^1, \lambda^1, \alpha^1) \in M$ and $(x^2, \lambda^2, \alpha^2) \in M$. Let $(x^1, \lambda^1, \alpha^1)$ be a local minimum point of g_{α^*}, subject to $h(x) = 0$, meeting the second-order sufficient condition, and let $(x^2, \lambda^2, \alpha^2)$ be a saddle point of g_{α^*}, subject to $h(x) = 0$, with regular Hessian $\nabla^2 \mathrm{L}_{\alpha^2}(\mathrm{x}^2)|_{\mathrm{span}\{\nabla h_1(x^2),\ldots,\nabla h_m(x^2)\}^\perp}$. Let us assume that both points can be connected by a continuous curve

$$\tau: \mathbb{R} \supset [0, 1] \to M,\ t \mapsto (x(t), \lambda(t), \alpha(t)),$$

with

$$\tau(0) = (x^1, \lambda^1, \alpha^1) \quad \text{and} \quad \tau(1) = (x^2, \lambda^2, \alpha^2),$$

where all $x(t)$, $t \in [0, 1]$, meet the constraint qualification (CQ). Calculating for each point $\tau(t)$ the $(n-m)$-tuple formed by the eigenvalues of the linear mappings $\nabla^2 L_{\alpha(t)}(x(t))|_{\mathrm{span}\{\nabla h_1(x(t)),\ldots,\nabla h_m(x(t))\}^\perp}$, one obtains a continuous curve $\tilde{\tau}: t \mapsto (\nu_1(t), \ldots, \nu_{n-m}(t))^T$ which corresponds to the curve τ. By assumption, $\nu_i(0) > 0$, $\forall i \in \{1, \ldots, n-m\}$, and $\exists j \in \{1, \ldots, n-m\}$ such that $\nu_j(1) < 0$. By the continuity of $\tilde{\tau}$, there must be a parameter value $t_0 \in [0, 1]$ with $\nu_j(t_0) = 0$. The point $\tau(t_0) \in M$, which can be looked upon as a transition point between an area of minima and an area of saddle points on M, meets none of the two sufficient criteria of Corollary 2.1.

Nonetheless, our plan to move around on the manifold M be means of a generalized continuation method requires generically that the rank condition (6) should also hold for such a point $\tau(t_0)$. Theorem 2.3 states that this is indeed the case: Points on M for which the eigenspace corresponding to the zero eigenvalue of $\nabla^2 L_{\alpha^*}(x^*)|_{S^\perp}$ does not vanish do meet the rank condition (6) if and only if none of the (nontrivial) vectors of the eigenspace is at the same time an element of the kernel of the linear mapping $f'(x^*)$. If the eigenspace is one-dimensional, this criterion can be checked easily: There has to be at least one single objective function f_i with $\nabla f_i(x^*)^T \cdot u \neq 0$, where u denotes the normalized eigenvector of the eigenvalue 0.

2.3. Special Class of Local Charts. Given a point $(x^*, \lambda^*, \alpha^*) \in M$, we want to investigate the neighborhood of this point on M. That is, we want to find other points of $M \cap U$, where $U \subset \mathbb{R}^{n+m+k}$ is an open neighborhood of $(x^*, \lambda^*, \alpha^*)$. The basic idea of our approach is to construct an appropriate local chart of $M \cap U$ and to generate points of $M \cap U$ by varying the chart parameters. A local chart φ of the C^1-submanifold $M \cap U$ of $\mathbb{R}^{n+m+k}$ is defined as a C^1-homeomorphism $\varphi: T \to V$ which maps an open subset

$T \subset \mathbb{R}^{k-1}$ onto an open neighborhood $V \subset (M \cap U)$ of the point $(x^*, \lambda^*, \alpha^*)$ and which meets the rank condition

$$\operatorname{rank} \varphi'(\xi) = k - 1, \qquad \forall \xi \in T.$$

Looking for guidelines for the construction of an appropriate local chart φ, first we note the natural requirement

$$\varphi(0) = (x^*, \lambda^*, \alpha^*).$$

The second construction principle arises from our intention to investigate the neighborhood V of $(x^*, \lambda^*, \alpha^*)$ along all directions without leaving $\varphi(T)$. Since the heuristic notion of a direction on V can be formalized naturally by means of a generalized local coordinate curve $\tau_t: [0, a) \to V$, $\gamma \mapsto \varphi(\gamma \cdot t)$, where $t \in \mathbb{R}^{k-1}$, $\|t\| = 1$, and $a \cdot t \in \partial T$ (the boundary of T), we are led to require that the infimum of the set of distances $\{\|p\| \mid p \in \partial T \subset \mathbb{R}^{k-1}\}$ between the origin $0 \in T$ and the boundary points of T should be as large as possible.

The two requirements stated above suggest that we introduce a coordinate system which is adapted to the local geometry of the manifold $M \cap U$. Assuming that $M \cap U$ is a $(k-1)$-dimensional C^1-submanifold of $\mathbb{R}^{n+m+k}$, we define a local chart φ by the following procedure:

(a) Decompose the vector space $\mathbb{R}^{n+m+k}$ into the $(k-1)$-dimensional subspace $T_{(x^*,\lambda^*,\alpha^*)}(M \cap U)$, denoting the tangent space of $M \cap U$ in $(x^*, \lambda^*, \alpha^*)$, and its orthogonal complement $(T_{(x^*,\lambda^*,\alpha^*)}(M \cap U))^{\perp}$.

(b) Construct an orthonormal basis $\{q_1, \ldots, q_{n+m+k}\}$ of $\mathbb{R}^{n+m+k}$ such that

$$\operatorname{span}\{q_1, \ldots, q_{k-1}\} = T_{(x^*,\lambda^*,\alpha^*)}(M \cap U)$$

and

$$\operatorname{span}\{q_k, \ldots, q_{n+m+k}\} = (T_{(x^*,\lambda^*,\alpha^*)}(M \cap U))^{\perp},$$

and attach this basis to the point $(x^*, \lambda^*, \alpha^*)$.

(c) Project a point $(x, \lambda, \alpha) \in M \cap U$, which is to be characterized by means of the local chart φ, onto the linear subspace $T_{(x^*,\lambda^*,\alpha^*)}(M \cap U)$, which has been attached to $(x^*, \lambda^*, \alpha^*)$, and record the coordinates ξ of the projected vector with respect to the basis $\{q_1, \ldots, q_{k-1}\}$. Taking ξ as the chart parameter results in a local chart φ of the form

$$\varphi: \xi \mapsto (x^*, \lambda^*, \alpha^*) + Q \begin{bmatrix} \xi \\ \eta(\xi) \end{bmatrix}, \tag{14}$$

where

$$Q := (q_1 | \ldots | q_{n+m+k})$$

is the orthonormal matrix formed by the basis vectors q_i and η denotes a continuously differentiable mapping,

$$\eta: \mathbb{R}^{k-1} \supseteq T \to \mathbb{R}^{n+m+1}, \qquad \text{with } \eta(0) = 0 \quad \text{and} \quad (\partial\eta/\partial\xi)(0) = 0.$$

The following theorem guarantees the existence of such a local chart.

Theorem 2.4. Consider a point $(x^*, \lambda^*, \alpha^*) \in M$ and assume that there exists an open neighborhood $U \subset \mathbb{R}^{n+m+k}$ of $(x^*, \lambda^*, \alpha^*)$ such that $M \cap U$ is a $(k-1)$-dimensional C^1-submanifold of $\mathbb{R}^{n+m+k}$. Furthermore, let $\{q_1, \ldots, q_{n+m+k}\}$ be an orthonormal basis of $\mathbb{R}^{n+m+k}$ such that $\operatorname{span}\{q_1, \ldots, q_{k-1}\} = T_{(x^*,\lambda^*,\alpha^*)}(M \cap U)$, and let $Q := (q_1 | \ldots | q_{n+m+k})$ denote the orthogonal matrix formed by the basis vectors q_i. Then, there exists an open neighborhood $T \subset \mathbb{R}^{k-1}$ of the origin $0 \in \mathbb{R}^{k-1}$, an open neighborhood $V \subset (M \cap U)$ of $(x^*, \lambda^*, \alpha^*)$, and a local chart of the form

$$\varphi: \begin{cases} T \to V, \\ \xi \mapsto (x^*, \lambda^*, \alpha^*) + Q \begin{bmatrix} \xi \\ \eta(\xi) \end{bmatrix}, \end{cases} \tag{15}$$

where

$$\eta(0) = 0 \quad \text{and} \quad (\partial\eta/\partial\xi)(0) = 0. \tag{16}$$

Proof. Let $\bar{U} \subseteq U$ be a neighborhood of $(x^*, \lambda^*, \alpha^*)$ such that $\bar{\alpha}_i > 0$ for all $i \in \{1, \ldots, k\}$ and $(\bar{x}, \bar{\lambda}, \bar{\alpha}) \in \bar{U}$, let (x, λ, α) be an arbitrary point of $M \cap U$, and let us denote the coordinates of $(x, \lambda, \alpha) - (x^*, \lambda^*, \alpha^*)$ with respect to the basis $\{q_1, \ldots, q_{n+m+k}\}$ by $(\xi, \mu)^T$, $\xi \in \mathbb{R}^{k-1}$, $\mu \in \mathbb{R}^{n+m+1}$; i.e.,

$$(x, \lambda, \alpha) = (x^*, \lambda^*, \alpha^*) + Q \begin{bmatrix} \xi \\ \mu \end{bmatrix}. \tag{17}$$

The inverse image of $\bar{U}$ with respect to this coordinate transformation is an open neighborhood $\tilde{U}$ of the origin in the space of the (ξ, μ)-coordinates. A point of $\mathbb{R}^{n+m+k}$ solves the equation $F(x, \lambda, \alpha) = 0$ if and only if its (ξ, μ)-coordinates solve the following equation:

$$\begin{aligned} \tilde{F}(\xi, \mu) &:= F(x(\xi, \mu), \lambda(\xi, \mu), \alpha(\xi, \mu)) \\ &= F\left[(x^*, \lambda^*, \alpha^*) + Q \begin{bmatrix} \xi \\ \mu \end{bmatrix}\right] = 0. \end{aligned} \tag{18}$$

Describing the set of solutions of (18) by

$$\tilde{M} := \{(\xi, \mu) \in \mathbb{R}^{n+m+k} \mid \tilde{F}(\xi, \mu) = 0\},$$

we can conclude that the coordinate transformation (17) establishes a diffeomorphism between the C^1-manifolds $\tilde{M}\tilde{U}$ and $M \cap \tilde{U}$.

Our next step is to construct a local chart of $\tilde{M}\tilde{U}$.

The Jacobian matrix of $\tilde{F}$, evaluated at the point $(\xi, \mu) = 0$, is given by

$$\tilde{F}'|_{(\xi,\mu)=0} \equiv \partial\tilde{F}/\partial(\xi, \mu)|_{(\xi,\mu)=0} = F'(x^*, \lambda^*, \alpha^*)Q. \tag{19}$$

Since the ith row of $F'(x^*, \lambda^*, \alpha^*)$ can be written as $\nabla_{(x,\lambda,\alpha)}F_i(x^*, \lambda^*, \alpha^*)^T$, where $\nabla_{(x,\lambda,\alpha)} \equiv (\partial/\partial x, \partial/\partial\lambda, \partial/\partial\alpha)$, the rows of $F'(x^*, \lambda^*, \alpha^*)$ form a base of the subspace $(T_{(x^*,\lambda^*,\alpha^*)}(M \cap U))^{\perp}$. For any $l \in \{k, \ldots, n+m+k\}$, the lth column of the matrix $F'(x^*, \lambda^*, \alpha^*)Q$ can be interpreted as the tuple of coefficients of the vector $q_l \in [T_{(x^*,\lambda^*,\alpha^*)}(M \cap U)]^{\perp}$ with respect to the basis $\{\nabla_{(x,\lambda,\alpha)}F_1, \ldots, \nabla_{(x,\lambda,\alpha)}F_{n+m+1}\}$. As the linear independence of the vectors $\{q_k, \ldots, q_{n+m+k}\}$ is preserved by this change of basis, the last $n+m+1$ columns of the matrix $\tilde{F}'|_{(\xi,\mu)=0} = F'(x^*, \lambda^*, \alpha^*)Q$ are linearly independent vectors, and we obtain

$$\operatorname{rank}(\partial\tilde{F}/\partial\mu)_{(\xi,\mu)=0} = n + m + 1. \tag{20}$$

Therefore, according to the implicit function theorem, there exist an open neighborhood $T \subset \mathbb{R}^{k-1}$ of the origin $0 \in \mathbb{R}^{k-1}$, an open neighborhood $W \subset \mathbb{R}^{n+m+1}$ of the origin $0 \in \mathbb{R}^{n+m+1}$, and a continuously differentiable function $\eta: T \to W$ such that Eq. (18) has exactly one solution $(\xi, \mu) = (\xi, \eta(\xi))$ for each $\xi \in T$. Since the point $(0, 0)$ solves (18), we have $\eta(0) = 0$.

The set $\tilde{V} := \tilde{M} \cap (T \times W)$ is an open neighborhood of the origin $0 \in (\tilde{M} \cap \tilde{U}) \subset \mathbb{R}^{n+m+k}$. We choose the neighborhoods T and W small enough to ensure that $T \times W \subset \tilde{U}$. As a consequence, $\tilde{V} \subset (\tilde{M} \cap \tilde{U})$, and the mapping

$$\tilde{\varphi}: \begin{cases} T \to \tilde{V}, \\ \xi \mapsto \begin{bmatrix} \xi \\ \eta(\xi) \end{bmatrix}, \end{cases} \tag{21}$$

is a local chart of the C^1-manifold $\tilde{M} \cap \tilde{U}$. Composing $\tilde{\varphi}$ with the coordinate transformation (17) and defining V as the image of $\tilde{V}$ with respect to the coordinate transformation, we obtain a mapping φ of the form (15) as a chart of the C^1-manifold $M \cap U$.

In order to verify the second equation of (16), we write the Jacobian matrix of $\eta(\xi)$ at the point $\xi = 0$, as it is given by the implicit function theorem,

$$(\partial\eta/\partial\xi)(0) = -[(\partial\tilde{F}/\partial\eta)_{(\xi,\eta(\xi))=0}]^{-1}(\partial\tilde{F}/\partial\xi)_{(\xi,\eta(\xi))=0}. \tag{22}$$

As a result of (19), the matrix $(\partial \tilde{F}/\partial \xi)_{(\xi,\eta(\xi))=0}$ consists of the first $(k-1)$ columns of the matrix $F'(x^*, \lambda^*, \alpha^*)Q$. Since, by construction of the basis vectors $\{q_1, \ldots, q_{k-1}\}$,

$$\nabla_{(x,\lambda,\alpha)} F_i(x^*, \lambda^*, \alpha^*)^T q_j = 0,$$

$$\text{for all } i \in \{1, \ldots, n+m+1\} \text{ and } j \in \{1, \ldots, k-1\},$$

all these columns are null vectors, and (16) is proven. □

Two remarks are to be made regarding the feature $(\partial\eta/\partial\xi)(0) = 0$ of our local chart φ.

First, we note that the boundary of T (the domain of φ) is reached when an element of the matrix function $\partial\eta/\partial\xi$ diverges toward $+\infty$ or $-\infty$. Having only information about the tangent space of $M \cap U$ at our disposal, the property $(\partial\eta/\partial\xi)(0) = 0$ is the best measure that we can take to push such divergences and thus the boundary points of T as far away from the origin as possible. Second, $(\partial\eta/\partial\xi)(0) = 0$ is the decisive feature of our local chart on which the homogeneous discretization of the Pareto set is based; see Section 3.2 below.

3. Generalized Homotopy Method

3.1. Strategy. As mentioned earlier, our basic strategy to generate points on M in the neighborhood of some given point $(x^*, \lambda^*, \alpha^*) \in M$ is to choose a set of points $\xi_{(i)}$ from $T \subset \mathbb{R}^{k-1}$, the domain of φ, and to calculate $\varphi(\xi_{(i)})$ for all points $\xi_{(i)}$ numerically. Computing $\varphi(\xi_{(i)})$ is done in two steps.

(A) In this step, we calculate the projection $\varphi^P(\xi_{(i)})$ of $\varphi(\xi_{(i)})$ onto the tangent space $T_{(x^*,\lambda^*,\alpha^*)}M$. By construction of the chart φ, $\varphi^P(\xi_{(i)})$ is given by

$$\varphi^P(\xi_{(i)}) = (x^*, \lambda^*, \alpha^*) + (q_1 \ldots q_{k-1})\xi_{(i)}, \tag{23}$$

where $\{q_1, \ldots, q_{k-1}\}$ denotes an orthonormal basis of $T_{(x^*,\lambda^*,\alpha^*)}M$.

(B) Starting from the point $\varphi^P(\xi_{(i)})$ on the tangent space, this step is meant to result in a point on the manifold M itself. In order to lie on M, the point $\varphi(\xi_{(i)})$ has to solve Eq. (4); i.e.,

$$F(\varphi(\xi_{(i)})) = F\left[(x^*, \lambda^*, \alpha^*) + Q\begin{bmatrix}\xi_{(i)} \\ \eta(\xi_{(i)})\end{bmatrix}\right] = 0. \tag{24}$$

(24) is a system of $n+m+1$ equations for the $n+m+1$ unknown quantities $\eta(\xi_{(i)}) =: \eta_{(i)}$ and, due to the assumption $\xi_{(i)} \in T$, is guaranteed to have a solution. Step B consists of the numerical solution of (24) with the help of the Newton method. Here, the value 0 of the η^*-coordinate, which corresponds to the projection $\varphi^P(\xi_{(i)})$, serves as a starting point for the Newton method.

When it is considered from the viewpoint of numerical mathematics, this strategy turns out to describe a homotopy approach which has been generalized to the case of multidimensional homotopy parameters. The predictor of the homotopy method is formed by Step (A); the corrector is formed by Step (B).

3.2. Uniform Spread of Pareto Points. Any numerical method solving (MOP) will be able to compute only a limited number of Pareto points or candidates. Thus, it becomes crucial to have these points spread as uniformly as possible, so that a good approximation of the whole Pareto surface is obtained and clusters of points in certain areas, which fail to provide a good idea of the entire shape, are avoided. In the sequel, we will show that the proposed homotopy method is capable of producing a homogeneous discretization of the Pareto surface.

First, we investigate the distance in objective space between points computed by the homotopy algorithm. Assume that a point $(x^*, \lambda^*, \alpha^*) \in M$ is given and that φ is a local chart as defined in (14). We choose a chart parameter vector $\xi_{(i)} := \delta_{(i)} \cdot e_i$, where $\delta_{(i)} \in \mathbb{R}$ and $|\delta_{(i)}| \ll 1$, and where e_i denotes the ith unit vector in $\mathbb{R}^{k-1}$, and calculate the Euclidean distance ρ between the points $f(x^*)$ and $f(P_x \varphi(\xi_{(i)}))$ in objective space. Here, P_x denotes the projector onto x-space; i.e.,

$$P_x(x, \lambda, \alpha) = x.$$

The distance ρ can be made a function of $\delta_{(i)}$ by defining

$$\rho(\delta_{(i)}) := \| f(x^*) - f(P_x \varphi(\delta_{(i)} \cdot e_i)) \| \equiv \| f(x^*) - \tilde{f}(\delta_{(i)}) \|, \tag{25}$$

where the mapping $\tilde{f}$ is defined as

$$\tilde{f}: \mathbb{R} \to \mathbb{R}^k, \qquad \delta_{(i)} \mapsto f(P_x \varphi(\delta_{(i)} \cdot e_i)).$$

Computing the Taylor series expansion of $\rho(\delta_{(i)})$ near the point $\delta_{(i)}^0 = 0$ results in

$$\tilde{f}(\delta_{(i)}) = f(x^*) + \delta_{(i)} \cdot \begin{bmatrix} d\tilde{f}_1/d\delta_{(i)} \\ \vdots \\ d\tilde{f}_k/d\delta_{(i)} \end{bmatrix}_{\delta_{(i)}=0} + o(\delta_{(i)}), \tag{26}$$

$$(d\tilde{f}_j/d\delta_{(i)})_{\delta_{(i)}=0} = \nabla f_j(x^*)^T (dx/d\delta_{(i)})_{\delta_{(i)}=0}, \qquad j = 1, \ldots, k, \tag{27}$$

$$(dx/d\delta_{(i)})_{\delta_{(i)}=0} = \bar{Q} \begin{bmatrix} d(\delta_{(i)} \cdot e_i)/d\delta_{(i)} \\ d\eta(\delta_{(i)} \cdot e_i)/d\delta_{(i)} \end{bmatrix}_{\delta_{(i)}=0} = \bar{Q} \begin{bmatrix} e_i \\ 0 \end{bmatrix} = \bar{q}_i, \tag{28}$$

where $\bar{Q}$ is the submatrix of Q formed by the first n rows, $\bar{q}_i \in \mathbb{R}^n$ is the vector formed by the first n elements of the basis vector q_i (see Section 2.3), and $o(\delta_{(i)})$ denotes a mapping $g: \mathbb{R} \to \mathbb{R}^k$ with $g(0) = 0$ and

$$\lim_{\delta_{(i)} \to 0,\ \delta_{(i)} \neq 0} g_j(\delta_{(i)})/\delta_{(i)} = 0, \qquad \forall j = 1, \ldots, k.$$

It should be emphasized that the second identity in (28) is a consequence of $(\partial\eta/\partial\xi)(0) = 0$. Inserting (28) into (27) and the resulting equation into (26) gives

$$\tilde{f}(\delta_{(i)}) = f(x^*) + f'(x^*)\bar{q}_i \cdot \delta_{(i)} + o(\delta_{(i)}), \tag{29}$$

where f' denotes the Jacobian matrix of f. With the help of the argument given in Remark 3.1, we obtain

$$\rho(\delta_{(i)}) = \| f'(x^*)\bar{q}_i \| \cdot |\delta_{(i)}| + o(\delta_{(i)}). \tag{30}$$

Now, we are prepared to put our intention to produce a uniform spread of Pareto points in concrete terms. Assume again that a point $(x^*, \lambda^*, \alpha^*) \in M$ is given and that the homotopy algorithm is to compute further points $(x_{(i)}, \lambda_{(i)}, \alpha_{(i)}) \in M$ in the neighborhood of $(x^*, \lambda^*, \alpha^*)$. In order to obtain a uniform spread in objective space, the user of the algorithm should be able to predetermine the Euclidean distance $c \in \mathbb{R}^+$ between $f(x_{(i)})$ and $f(x^*)$; i.e.

$$\| f(x_{(i)}) - f(x^*) \| = c.$$

In the framework of a linear approximation, which is close to reality for small stepsizes $|\delta_{(i)}| \ll 1$, this requirement can be fulfilled due to (30) by choosing the chart parameter vectors $\xi_{(i)}$ as $\xi_{(i)} = \delta_{(i)} \cdot e_i$, $i = 1, \ldots, k-1$, with

$$\delta_{(i)} = c/\| f'(x^*)\bar{q}_i \|. \tag{31}$$

Thus, the discretization of the Pareto surface in objective space can be well controlled by an appropriate rescaling of the coordinate axes in the space of the ξ-parameters.

Remark 3.1. In order to obtain Eq. (30), we state first that

$$\|o(\delta_{(i)})\| = o(\delta_{(i)}). \tag{32}$$

This is true, since (32) is another way of writing

$$\lim_{\delta_{(i)} \to 0,\, \delta_{(i)} \neq 0} \left(\sum_{j=1}^{k} g_j(\delta_{(i)})^2 \right)^{1/2} \Big/ \delta_{(i)} = 0,$$

and since

$$\lim_{\delta_{(i)} \to 0,\, \delta_{(i)} \neq 0} \left(\sum_{j=1}^{k} g_j(b_{(i)})^2 \right)^{1/2} \Big/ \delta_{(i)} = \lim_{\delta_{(i)} \to 0,\, \delta_{(i)} \neq 0} \left(\sum_{j=1}^{k} (g_j(\delta_{(i)})/\delta_{(i)})^2 \right)^{1/2}$$

and

$$\lim_{\delta_{(i)} \to 0,\, \delta_{(i)} \neq 0} g_j(\delta_{(i)})/\delta_{(i)} = 0, \qquad \forall j = 1, \ldots, k.$$

Now, we insert (29) into (25) and get

$$\rho(\delta_{(i)}) = \| f'(x^*)\bar{q}_i \cdot \delta_{(i)} + o(\delta_{(i)}) \|. \tag{33}$$

The triangle axiom allows the conclusion

$$\left| \| f'(x^*)\bar{q}_i \cdot \delta_{(i)} + o(\delta_{(i)}) \| - \| f'(x^*)\bar{q}_i \cdot \delta_{(i)} \| \right| \leq \|o(\delta_{(i)})\|, \tag{34}$$

from which (30) follows immediately with the help of (32).

3.3. Formulation of the Algorithm. The following algorithm describes the numerical computation of a set of candidates for Pareto optimal solutions.

Step 1. A point $(x^*, \lambda^*, \alpha^*) \in M$ is selected to serve as a starting point of the next homotopy step. When the algorithm is started and no homotopy step has yet been performed, we obtain a point $(x^*, \lambda^*, \alpha^*)$ by choosing a weight vector $\alpha^* \in \mathbb{R}^k$, with $\alpha_i > 0$ for $i = 1, \ldots, k$ and $\sum_{i=1}^{k} \alpha_i^* = 1$, and solving the scalar-valued optimization problem minimize g_{α^*}, subject to $h(x) = 0$, by means of some state-of-the-art optimization technique, for example, sequential quadratic programming; see e.g. Ref. 10. Once the homotopy algorithm has been started, arbitrary points on M which have been generated by the algorithm may be chosen as new starting points $(x^*, \lambda^*, \alpha^*)$.

Step 2. Compute the Jacobian matrix F' of F at the point $(x^*, \lambda^*, \alpha^*)$ according to (9).

Step 3. Calculate a QR-factorization of the matrix $(F'(x^*, \lambda^*, \alpha^*))^T$ by means of Householder reflections. This factorization can

be performed for any value of rank $(F'(x^*, \lambda^*, \alpha^*))^T$. It results in

$$(F'(x^*, \lambda^*, \alpha^*))^T = \tilde{Q}R,$$

where $\tilde{Q} \in \mathbb{R}^{(n+m+k)\times(n+m+k)}$ is an orthonormal matrix and

$$R = \begin{bmatrix} R_1 \\ 0 \end{bmatrix} \in \mathbb{R}^{(n+m+k)\times(n+m+1)},$$

$R_1 \in \mathbb{R}^{(n+m+1)\times(n+m+1)}$ being an upper triangular matrix.

Step 4. The diagonal elements of R_1 give information about the rank of $F'(x^*, \lambda^*, \alpha^*)$,

$$\text{rank } F'(x^*, \lambda^*, \alpha^*) = n + m + 1,$$

if and only if $(R_1)_{jj} \neq 0$, for all $j = 1, \ldots, n+m+1$.

Therefore, we test the fulfillment of the rank condition (6) by checking numerically whether $|(R_1)_{jj}| > s$ holds for all $j = 1, \ldots, n+m+1$, where $s \in \mathbb{R}^+$ is some numerical threshold. If the rank condition is not met, the point $(x^*, \lambda^*, \alpha^*)$ cannot serve as a starting point for a homotopy step, and we have to go back to Step 1.

Step 5. The orthonormal matrix $\tilde{Q}$ obtained by Step 3 may be written as

$$\tilde{Q} = (\tilde{Q}_1 | \tilde{Q}_2),$$

where $\tilde{Q}_1 \in \mathbb{R}^{(n+m+k)\times(n+m+1)}$ and $\tilde{Q}_2 \in \mathbb{R}^{(n+m+k)\times(k-1)}$.

Since the column vectors of $\tilde{Q}_1$ span $(T_{(x^*,\lambda^*,\alpha^*)}M)^{\perp}$, and since the column vectors of $\tilde{Q}_2$ span $T_{(x^*,\lambda^*,\alpha^*)}M$, we obtain the orthonormal matrix Q required for the local chart φ [see Eq. (14)] by changing the sequence of the two submatrices $\tilde{Q}_1$ and $\tilde{Q}_2$; i.e.,

$$Q = (\tilde{Q}_2 | \tilde{Q}_1).$$

Step 6. Generate a set of chart parameter vectors $\{\xi_{(i)}\}$ labeled by an index set I. Let us assume that each point $x_{(i)}$ computed by the homotopy algorithm is supposed to have a given distance $c \in \mathbb{R}^+$ in objective space from the starting point x^*; i.e.,

$$\| f(x_{(i)}) - f(x^*) \| \approx c.$$

This requirement can be fulfilled by choosing $I = \{1, \ldots, k-1\}$ as the index set and $\xi_{(i)} = [c/\| f'(x^*)\bar{q}_i \|]e_i$ as the ith chart parameter vector; see Section 3.2.

Step 7. Carry out Steps 8 to 10 for all $i \in I$.

Step 8. Calculate the predictor $\varphi^P(\xi_{(i)})$ according to Step (A), Section 3.1.

Step 9. Compute the corrector according to Step (B), Section 3.1. After a given maximum number $l_{\max}$ of Newton iterations, if the norm of the residual vector

$$F\left[(x^*, \lambda^*, \alpha^*) + Q\begin{bmatrix}\xi_{(i)} \\ \eta_{(i)}^{[l_{\max}]}\end{bmatrix}\right]$$

of the Newton sequence has not fallen below some given error threshold, we assume that the Newton algorithm does not converge. From that, we conclude that the predictor $\varphi^P(\xi_{(i)})$ is too far away from the manifold M; i.e., the stepsize of the predictor step has been chosen too large in view of the local curvature of M. Therefore, we divide the chart parameter vector $\xi_{(i)}$ by two and go back to the predictor Step 8. Thus, the convergence behavior of the Newton algorithm is used as a sensor for the stepsize control of the individual homotopy steps.

Step 10. Check whether the calculated point $\varphi(\xi_{(i)})$ is really an element of M. For that purpose, we have to examine whether all elements of the vector $P_\alpha \varphi(\xi_{(i)})$, where P_α denotes the projector onto the α-space [i.e., $P_\alpha(x, \lambda, \alpha) = \alpha$], are positive. If that is not the case, we divide the chart parameter $\xi_{(i)}$ by two and go back to the predictor Step 8.

4. Numerical Results

Example 4.1. Academic Example. Consider the following unconstrained (MOP): $\min_{x \in \mathbb{R}^2} \{f(x)\}$, where f is defined as

$$f: \begin{cases} \mathbb{R}^2 \to \mathbb{R}^2, \\ x \mapsto \begin{bmatrix} \cos(a(x)) \cdot b(x) \\ \sin(a(x)) \cdot b(x) \end{bmatrix}, \end{cases} \tag{35a}$$

with

$$a(x) := (2\pi/360)[a_c + a_1 \sin(2\pi x_1) + a_2 \sin(2\pi x_2)], \tag{35b}$$

$$b(x) := 1 + d\cos(2\pi x_1). \tag{35c}$$

For the numerical calculations, the constant parameters a_c, a_1, a_2, d have been chosen as

$$a_c = 45, \qquad a_1 = 40, \qquad a_2 = 25, \qquad d = 0.5.$$

Since f is a periodic function of period 1 with respect to both arguments, a good representation of the image set $f(\mathbb{R}^2)$ can be obtained by discretizing the square $[0, 1] \times [0, 1]$ by a fine grid and plotting all the image points. The result is shown in Fig. 1(a).

Now, we start to calculate the curve of efficient points numerically by the homotopy method. In order to get a starting point $(x^*, \alpha^*) \in M$, we choose $\alpha^* = (0.5, 0.5)^T$ and minimize g_{α^*} by means of the Newton method. In Fig. 1(b), $f(x^*)$ is symbolized by +. In both directions, we perform 300 homotopy steps with a fixed stepsize $\xi_0 = 0.06$. Reversing the direction from one homotopy step to the other is prevented by the following measure. For each step, we check whether the condition

$$[(x, \alpha)_{(l)} - (x, \alpha)_{(l-1)}]^T \cdot q \geq 0$$

is met, where l denotes the label of the homotopy step and q is the numerically computed basis vector of the tangent $T_{(x,\alpha)_{(l)}} M$. If that is not the case, the chart parameter ξ_{l+1} is chosen to be $\xi_{l+1} = -\xi_0$ instead of $+\xi_0$. Figure 1(b) shows the resulting points in objective space. We call the collection of these points Candidate Set 1. The comparison with Fig. 1(a) teaches that Candidate Set 1 contains only a subset of the Pareto curve.[4] Furthermore, the spread of the computed points on the Pareto curve is uneven.

In order to remedy the latter drawback, we replace the fixed stepsize ξ_0 by a step-size control according to the rescaling rule (31). As shown in Fig. 1(c), this improvement indeed yields an even spread of Pareto candidates. The stepsize control reduces the number of homotopy steps which are needed for an adequate resolution of the Pareto curve significantly (100 steps instead of 300). In order to obtain the rest of the Pareto curve, we repeat the procedure two more times choosing

$$(x^*, \alpha^*) = (0.75, 0.6, 0.5, 0.5) \quad \text{and} \quad (x^*, \alpha^*) = (0.5, 0.5, 0.5, 0.5)$$

as starting points. The resulting sets of Pareto candidates are shown in Figs. 1(d) and (e). Figure 1(f) presents the union of the three numerically computed candidate sets. As can be seen by comparing Figs. 1(a) and 1(f), this sum-set includes the whole Pareto curve. MOP 1 represents a nontrivial class of (MOP)s, where the set of Pareto optimal solutions is composed of several candidate manifolds.

[4]Since we have allowed the α-components to be negative, not all points of Candidate Set 1 are really efficient.

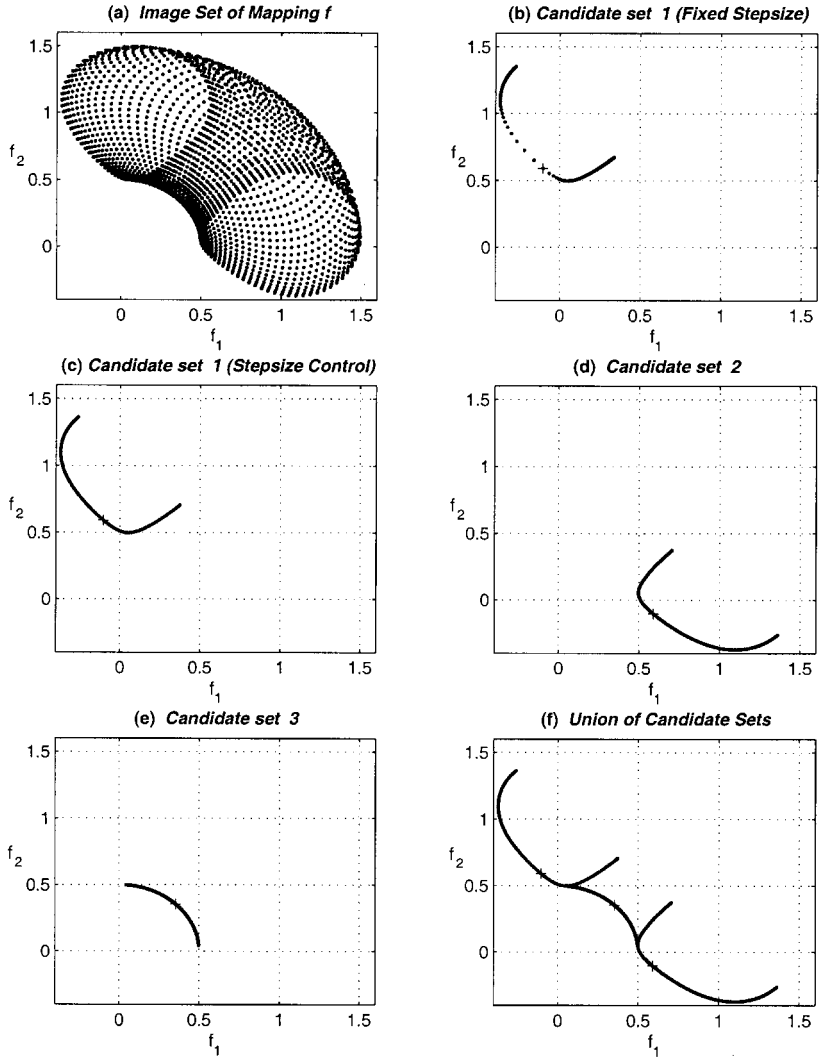

Fig. 1. Candidate sets for Pareto optimal solutions in objective space. Candidate Set 1 has been computed first (b) without rescaling of the chart parameter ξ and then (c) with rescaling.

In Section 2.1, we have stated that for nonconvex image sets $f(R)$, saddle points of linear combinations g_α may form an essential part of the Pareto set. MOP 1 can serve as a piece of evidence for this assertion, since Candidate Set 3 consists of saddle points. This can be gathered from Fig. 2

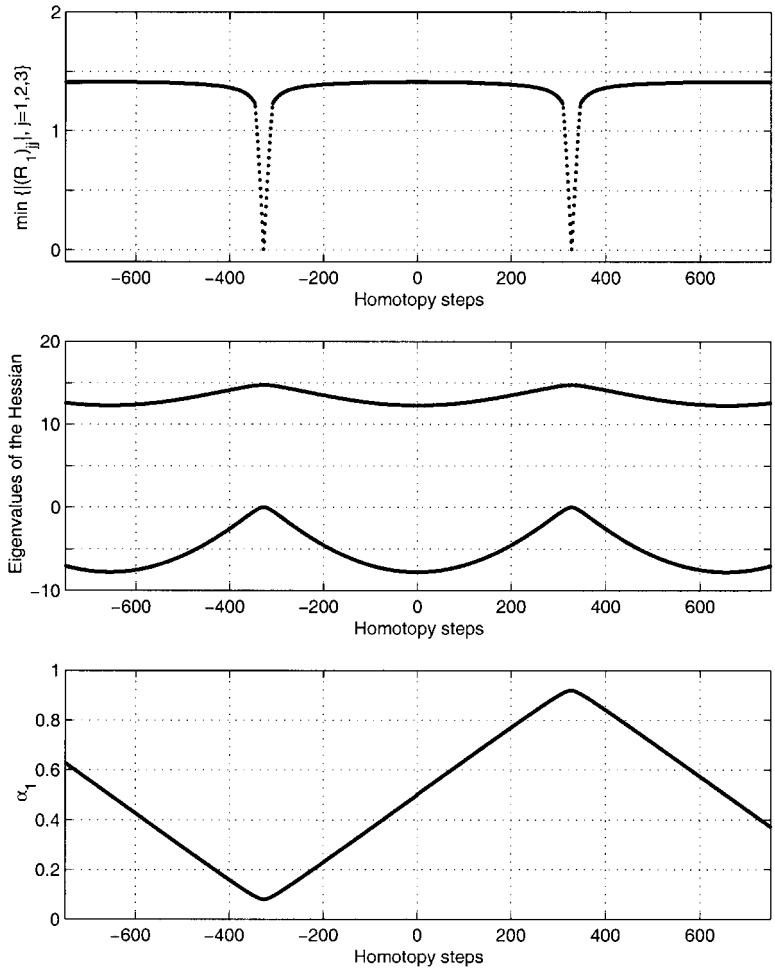

Fig. 2. Record of three quantities during the computation of Candidate Set 3. The iteration label 0 corresponds to the starting point (x^*, α^*), the sign of the labels indicates the direction of progress on the Pareto curve.

(middle part), where the egienvalues of the Hessian $\nabla^2 g_\alpha(x)$ are plotted against the iteration label of the homotopy steps. Since the Hessian is clearly indefinite (up to two points, see below) along the whole Candidate Set 3, the saddle point feature is proven.

Figure 1(f) reveals that Candidate Sets 3 and 1 as well as 3 and 2 intersect in the objective space. Plots of the corresponding inverse image

sets show that the candidate sets also intersect in (x, α)-space. At both intersection points, the set of solutions of (4) cannot be characterized locally by a chart and, thus, cannot be a one-dimensional C^1-manifold there. It can be inferred that the rank condition (6) cannot be met in these intersection points, i.e., that the Jacobian matrx $F'(x_{\text{intersect}}, \alpha_{\text{intersect}})$ has a rank smaller than the full rank 3. An important question is, whether our numerical homotopy method indicates clearly such a collapse of the dimension of the candidate manifold, which opens the possibility of a bifurcation. To answer this question, Fig. 2 (upper part) shows, for each homotopy step, the minimum of $|(R_1)_{jj}|, j \in \{1, 2, 3\}$, where R_1 denotes the triangular matrix resulting from the QR-factorization of $(F'(x, \alpha))^T$; see Steps 3 and 4 of the algorithm. Indeed, this minimum can be seen to be zero at two points, which are identified as the intersection points by looking at the corresponding α_1-values plotted in Fig. 2 (lower part).

The reason for the collapse of the rank of $F'(x, \alpha)$ at the two intersection points is revealed by Fig. 2 (middle part). At both points, an eigenvalue of the Hessian $\nabla^2 g_\alpha(x)$ is 0, and no gradient of a single objective is able to compensate for that rank deficit. According to Section 2.2, this is a nongeneric behavior. The following sample MOP 2 demonstrates the generic case, i.e., a zero eigenvalue of the Hessian which is not accompanied by a collapse of the dimension of the candidate manifold.

Example 4.2. Optimization of Power Plant Design. The design of combined cycle power plants is influenced strongly by three thermodynamical variables; the high-pressure, medium-pressure, and low-pressure pinchpoints. We will denote the triple of these design variables by $x \in \mathbb{R}^3$. Optimizing these design variables means to minimize the investment costs and simultaneously to maximize the efficiency (i.e., to minimize the negative efficiency) of the power plant. Since decreasing a pinchpoint improves the efficiency, but also increases the investment costs, we arrive at the unconstrained (MOP) $\min_{x \in \mathbb{R}^3} \{ f_{\text{power plant}}(x) \}$, where $f_{\text{power plant}}$ is defined as

$$f_{\text{power plant}} : \begin{cases} \mathbb{R}^3 \to \mathbb{R}^2, \\ x \mapsto \begin{bmatrix} \text{investment costs}(x) \\ -\text{efficiency}(x) \end{bmatrix}. \end{cases} \tag{36}$$

The evaluation of both individual objective functions is based on a simulation program which itself is based on a physical and economic model of the plant. In order to accelerate the evaluations, we approximate the function $f_{\text{power plant}}$ by a twice continuously differentiable mapping f_{approx}. This mapping is generated by defining a grid of technically sensible pinchpoint triples, evaluating the simulation model for each of these variable points,

and using the obtained data pairs $(x, f_{\text{power plant}}(x))$ for the training (i.e., parameter fitting by regression) of a neural 3-layer perceptron. The resulting mapping f_{approx} is used instead of $f_{\text{power plant}}$ in the following and is defined as

$$f_{j\,\text{approx}} = g_3 \circ g_2 \circ g_1, \qquad \text{for } j = 1, 2, \tag{37a}$$

where

$$g_1 : \begin{cases} \mathbb{R}^3 \to \mathbb{R}^{20}, \\ x \mapsto A_j \cdot x + b_j, \end{cases} \tag{37b}$$

$$g_2 : \begin{cases} \mathbb{R}^{20} \to \mathbb{R}^{20}, \\ (\ldots, x_i, \ldots)^T \mapsto (\ldots, \tanh(x_i), \ldots)^T, \end{cases} \tag{37c}$$

$$g_3 : \begin{cases} \mathbb{R}^{20} \to \mathbb{R}, \\ x \mapsto c_j^T \cdot x + d_j. \end{cases} \tag{37d}$$

Here, the matrix $A_j \in \mathbb{R}^{20\times 3}$, the vectors b_j, $c_j \in \mathbb{R}^{20}$, and the real number d_j represent the parameters (neural weights) obtained by the training procedure.

We start with a minimizer of a convex combination g_{α^*}, where $\alpha^* = (0.5, 0.5)^T$, and calculate a subset of the Pareto candidates as described in the previous example. The resulting points are shown in Fig. 3 both in the objective space and in a projection of the extended variable space into the (x_1, x_2)-plane. According to the lower subplot, the computed part of the curve of Pareto candidates has the shape of the letter z. Between the two points marked by $*$, whose common image is also marked by $*$ in the upper subplot, the curve consists obviously of points which are not globally efficient.

Figure 4 shows some quantities numerically computed plotted against the iteration label of the homotopy steps. The comparison between the lower subplot of Fig. 3 and the third subplot of Fig. 4 tells us that the transitions between the three parts of the z-curve occur near the 400th and near the 1000th homotopy step. As can be seen from the second subplot of Fig. 4, up to the first transition point all the eigenvalues of the Hessian matrices $\nabla^2 g_\alpha(x)$ are positive; therefore, the Pareto candidates are local minimizers of g_α. Between the two transition points, the curve consists of saddle points due to the indefiniteness of $\nabla^2 g_\alpha(x)$; beyond the second transition point, the curve is made up of minimizers of g_α again.

In both transition points, one eigenvalue of $\nabla^2 g_{\alpha_{\text{transition}}}(x_{\text{transition}})$ is zero. Nevertheless, the minimum of $|(R_1)_{jj}|$, $j \in \{1, 2, 3, 4\}$, which is shown in the first subplot of Fig. 4, is larger than the numerical threshold $s = 0.1$, which indicates clearly that the Jacobian matrix $F'(x_{\text{transition}}, \alpha_{\text{transition}})$ has the full

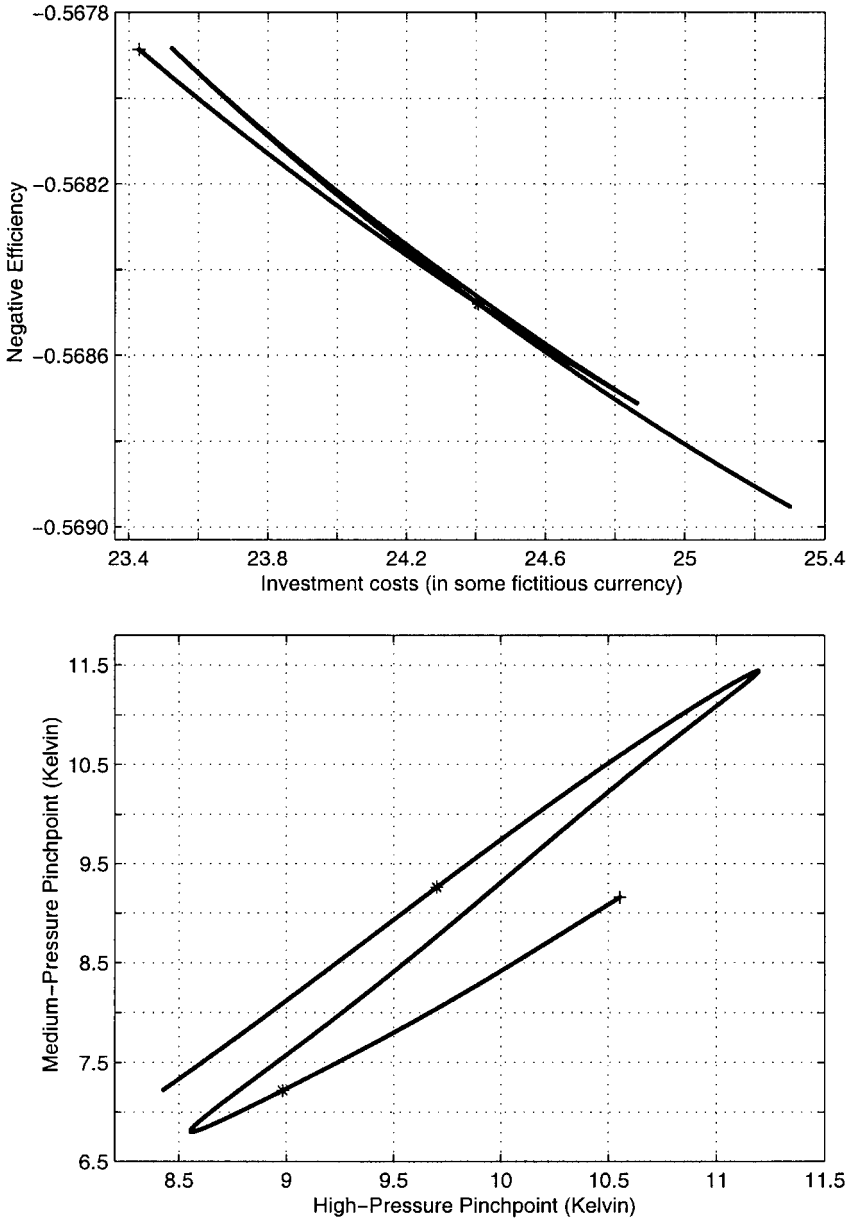

Fig. 3. Candidates for Pareto optimal solutions of power plant design in objective space (up) and variable space (down). The figure shows a detail of the whole curve of Pareto candidates which has mathematically interesting properties.

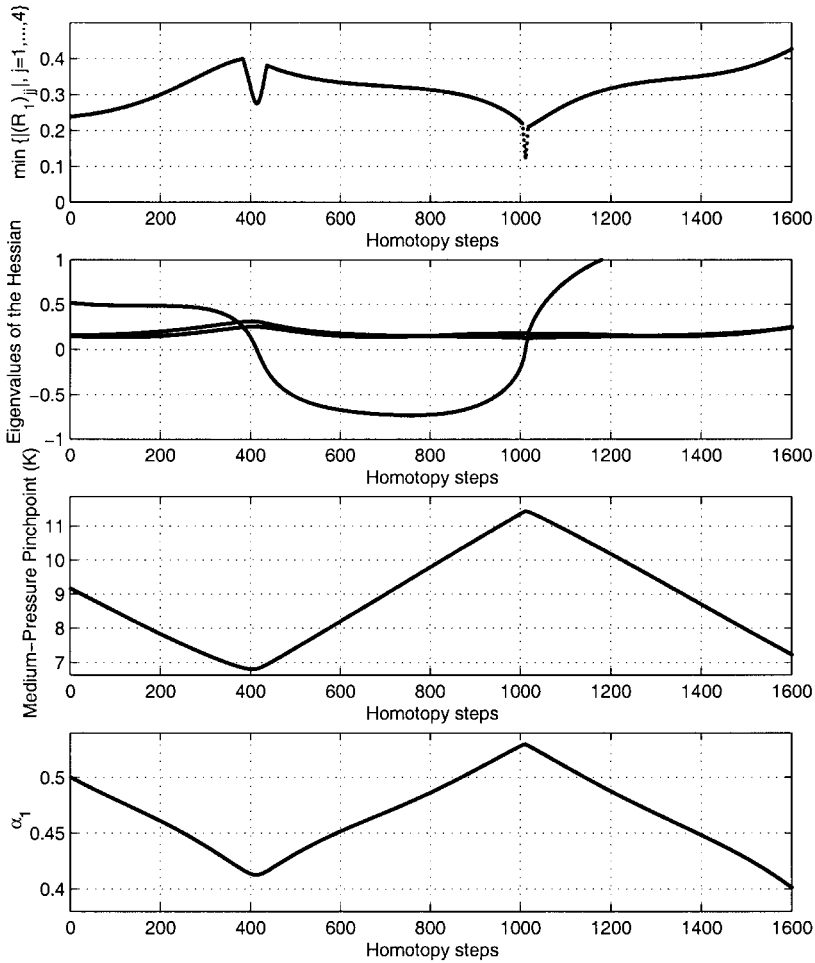

Fig. 4. Record of four quantities during the computation of the Pareto candidates shown in Fig. 3.

rank 4 and that the dimension of the candidate manifold does not change at these transition points (compare MOP 1).

The last two columns of the Jacobian matrix $F'(x_{\text{transition}}, \alpha_{\text{transition}})$, which make up the submatrix $(\partial F/\partial \alpha)(x_{\text{transition}}, \alpha_{\text{transition}})$, are needed to complete the rank of $F'(x_{\text{transition}}, \alpha_{\text{transition}})$ in both transition points. Therefore, due to the implicit function theorem, the candidate manifold M cannot be parametrized by α_1 in a neighborhood of these points; i.e., α_1 loses its

character of a potentially free homotopy parameter and becomes a dependent quantity. This implies that α_1 cannot be forced to progress to smaller and smaller values or larger and larger values beyond these transition points. The fourth subplot of Fig. 4 illustrates this behavior by showing that both zeros of an eigenvalue of the Hessian matrix are accompanied by an extremum of α_1.

References

1. STADLER, W., Editor, *Multicriteria Optimization in Engineering and in the Sciences*, Plenum Press, New York, NY, 1988.
2. ZADEH, L., *Optimality and Nonscalar-Valued Performance Criteria*, IEEE Transactions on Automatic Control, Vol. 8, pp. 59–60, 1963.
3. HAIMES, Y. Y., *Integrated System Identification and Optimization*, Control and Dynamic Systems: Advances in Theory and Applications, Edited by C. T. Leondes, Academic Press, New York, NY, Vol. 10, pp. 435–518, 1973.
4. DAS, I., and DENNIS, J., *Normal-Boundary Intersection: A New Method for Generating Pareto-Optimal Points in Multicriteria Optimization Problems*, Technical Report 96-11, Department of Computational and Applied Mathematics, Rice University, Houston, Texas, 1996.
5. DAS, I., *Nonlinear Multicriteria Optimization and Robust Optimality*, PhD Thesis, Rice University, Houston, Texas, 1997.
6. RAKOWSKA, J., HAFTKA, R. T., and WATSON, L. T., *Tracing the Efficient Curve for Multiobjective Control-Structure Optimization*, Computing Systems in Engineering, Vol. 2, pp. 461–471, 1991.
7. HILLERMEIER, C., *Eine Homotopiemethode zur Vektoroptimierung*, Habilitation Thesis, Technical University, München, Germany, 1999.
8. KUHN, H., and TUCKER, A., *Nonlinear Programming*, Proceedings of the 2nd Berkeley Symposium on Mathematical Statistics and Probability, Edited by J. Neyman, University of California, Berkeley, California, pp. 481–492, 1951.
9. LUENBERGER, D. G., *Linear and Nonlinear Programming*, Addison-Wesley Publishing Company, Reading, Massachusetts, 1984.
10. FLETCHER, R., *Practical Methods of Optimization*, John Wiley, New York, NY, 1987.